Materials Science and Engineering Publications   Materials Science and Engineering

11-2010

Compositional disorder, polar nanoregions and dipole dynamics in Pb(Mg1/3Nb2/3)O3-based relaxor ferroelectrics

Alexei A. Bokov
Simon Fraser University

Brian J. Rodriguez
University College Dublin

Xiaohui Zhao
Iowa State University, click@iastate.edu

Jae-Hyeon Ko
Hallym University

Stephen Jesse
Oak Ridge National Laboratory

Follow this and additional works at: http://lib.dr.iastate.edu/mse_pubs

See next page for additional authors

Part of the Ceramic Materials Commons, and the Physics Commons

Compositional disorder, polar nanoregions and dipole dynamics in Pb(Mg1/3Nb2/3)O3-based relaxor ferroelectrics

Abstract

The complex structure of relaxor ferroelectrics comprises polar nanoregions (PNRs) which appear upon cooling below the Burns temperature and quenched compositional (chemical) disorder. The relation between the polar nanostructure and compositionally ordered regions (CORs) often observed in relaxors has been the subject of extensive theoretical investigations; however, the experimental data, especially concerning $Pb(B'_{1/3}B''_{2/3})O_3$-type complex perovskite relaxors, are rather limited. In this paper, we analyse and discuss the results of our recent investigations of the morphology of CORs and the dynamics of PNRs in $Pb(Mg_{1/3}Nb_{2/3})O_3$ based solid solutions in which the degree of compositional disorder was varied by means of changing the composition and/or by means of high-temperature annealing. The samples were characterised using X-ray diffraction, transmission electron microscopy, piezoresponse force microscopy, Brillouin light scattering, dielectric spectroscopy, as well as by measuring pyroelectric effect and ferroelectric hysteresis loops. No influence of the size of CORs on the PNRs relaxation in the ergodic relaxor phase is found. Instead, the CORs size influences significantly the diffuseness of the transition from the field-induced ferroelectric phase to the ergodic relaxor state. The results are interpreted in the framework of a model suggesting the coexistence of static and dynamic PNRs in the ergodic relaxor phase.

Authors

Alexei A. Bokov, Brian J. Rodriguez, Xiaohui Zhao, Jae-Hyeon Ko, Stephen Jesse, Xifa Long, Weiguo Qu, Tae Hyun Kim, John D. Budai, Anna N. Morozovska, Seiji Kojima, Xiaoli Tan, Sergei V. Kalinin, and Zuo-Guang Ye

Compositional disorder, polar nanoregions and dipole dynamics in Pb(Mg$_{1/3}$Nb$_{2/3}$)O$_3$-based relaxor ferroelectrics

Alexei A. Bokov*,[I], Brian J. Rodriguez[II], Xiaohui Zhao[III], Jae-Hyeon Ko[IV], Stephen Jesse[V], Xifa Long[I], Weiguo Qu[III], Tae Hyun Kim[IV], John D. Budai[V], Anna N. Morozovska[VI], Seiji Kojima[VII], Xiaoli Tan[III], Sergei V. Kalinin[V] and Zuo-Guang Ye*,[I]

[I] Department of Chemistry and 4D LABS, Simon Fraser University, Burnaby, British Columbia V5A 1A6, Canada
[II] University College Dublin, Belfield, Dublin 4, Ireland
[III] Department of Materials Science and Engineering, Iowa State University, Ames, Iowa 50011, USA
[IV] Department of Physics, Hallym University, 39 Hallymdaehakgil, Chuncheon, Gangwondo 200-702, Republic of Korea
[V] Oak Ridge National Laboratory, Oak Ridge, Tennessee 37831, USA
[VI] V. Lashkaryov Institute of Semiconductor Physics, National Academy of Science of Ukraine, 41 Prospect Nauki, 03028 Kiev, Ukraine
[VII] Institute of Materials Science, University of Tsukuba, Tsukuba City, Ibaraki 305-8573, Japan

Abstract. The complex structure of relaxor ferroelectrics comprises polar nanoregions (PNRs) which appear upon cooling below the Burns temperature and quenched compositional (chemical) disorder. The relation between the polar nanostructure and compositionally ordered regions (CORs) often observed in relaxors has been the subject of extensive theoretical investigations; however, the experimental data, especially concerning Pb(B$'_{1/3}$B$''_{2/3}$)O$_3$-type complex perovskite relaxors, are rather limited. In this paper, we analyse and discuss the results of our recent investigations of the morphology of CORs and the dynamics of PNRs in Pb(Mg$_{1/3}$Nb$_{2/3}$)O$_3$-based solid solutions in which the degree of compositional disorder was varied by means of changing the composition and/or by means of high-temperature annealing. The samples were characterised using X-ray diffraction, transmission electron microscopy, piezo-response force microscopy, Brillouin light scattering, dielectric spectroscopy, as well as by measuring pyroelectric effect and ferroelectric hysteresis loops. No influence of the size of CORs on the PNRs relaxation in the ergodic relaxor phase is found. Instead, the CORs size influences significantly the diffuseness of the transition from the field-induced ferroelectric phase to the ergodic relaxor state. The results are interpreted in the framework of a model suggesting the coexistence of static and dynamic PNRs in the ergodic relaxor phase.

Introduction

The extraordinary properties of relaxor ferroelectrics which make possible their numerous technological appli-

cations are related to the unique sequence of phase transformations observed in these materials [1–3]. In contrast to normal ferroelectrics where the non-polar paraelectric phase transforms directly to the polar ferroelectric one at the Curie point (T_C), in relaxor ferroelectrics an intermediate ergodic relaxor phase is observed which appears upon cooling from the paraelectric phase at Burns temperature (T_B). The crystal may become ferroelectric only at $T_C \ll T_B$. For some compositions, however, the ferroelectric phase remains unattainable without the help of a strong enough external electric field, and the crystal transforms to a glassy nonergodic relaxor phase at a freezing temperature $T_f \ll T_B$. The main structural feature of the ergodic relaxor phase is the existence of small (few nanometres in size) islands in which the paraelectric structure is distorted so that a permanent local polarization appears. These islands, the so-called polar nanoregions (PNRs), are embedded into the non-polar matrix remaining from the paraelectric phase. In canonical relaxors the size of PNRs gradually increases with decreasing temperature and saturates at $T < T_f$. In those relaxors where a low-temperature ferroelectric phase exists, the PNRs develop into ferroelectric domains below T_C. The directions of PNR dipole moments are randomly different; therefore on the mesoscopic scales which are probed by conventional structural determination techniques (polarized light microscopy, X-ray or neutron diffraction) the crystal remains non-polar. The best-known example of canonical relaxor is Pb(Mg$_{1/3}$Nb$_{2/3}$)O$_3$ (PMN) with the perovskite structure (space group $Pm\bar{3}m$), $T_B \cong 630$ K and $T_f \cong 210$ K.

The mixture of polar and nonpolar regions is not the only type of nanoscale inhomogeneity observed in relaxors. The other type is related to the compositional (or chemical) disorder, that is, the disorder in the arrangement of different cations (*e.g.* Mg^{2+} and Nb^{5+} in PMN) on the equivalent lattice sites (*e.g.* the sites in the centres of oxygen octahedra of the perovskite structure). In PMN crystal this arrangement is random throughout the crystal except

* Correspondence authors (e-mail: abokov@sfu.ca; zye@sfu.ca)

in a number of small compositionally ordered nanoregions (CORs) in which the superstructure is formed so that the (111) planes filled by the Nb^{5+} cations alternate with the (111) planes filled by the mixture of Nb^{5+} and Mg^{2+} cations, giving rise to the doubling of the unit cell size and $Fm\bar{3}m$ space group inside CORs. The size of CORs in PMN is $2-5$ nm, *i.e.* approximately the same as the size of PNRs. In contrast to PNRs, however, the morphology of CORs in PMN (their dimensions and location and the degree of compositional order inside them) remains unchanged at all temperatures. In some other perovskite relaxors the COR morphology can be changed by means of high-temperature ($\sim 1000\,°C$) annealing and subsequent quenching or by variation of crystal growth conditions [4–6].

It was understood quite long ago that to account for the specific properties of relaxors such as the diffuse and extremely high peak in the temperature dependence of the dielectric constant, $\varepsilon(T)$, and the unusual dielectric dispersion, one needs to assume that the PNRs (or a large portion of them) are dynamic, *i.e.* their dipole moment directions vary due to the thermal motion. Different mechanisms of these variations were considered, including flipping among several directions allowed by the local symmetry [1] and structural rearrangements inside PNRs [7, 8]. Reorientations of the dipole moments of PNRs are believed to provide the main contribution to the dielectric relaxation in the ergodic relaxor phase. When temperature decreases the characteristic time of PNRs reorientations (and consequently the characteristic time of the dielectric relaxation) increases and finally diverges at T_f (glassy freezing), *i.e.* the PNRs become static at $T < T_f$ [9].

The connection between the relaxor state and the compositional disorder is evident: no relaxor ferroelectric behavior was observed among completely compositionally ordered crystals. However, the mechanisms by which compositional disorder destroys a normal ferroelectric phase and creates the relaxor state remain unclear. In particular, understanding the relation between PNRs and CORs is of great interest. It was suggested [2, 10] that CORs act as sites to localize the PNRs emerging below T_B and, therefore, the positions of these different types of nanoregions coincide, *i.e.* CORs and PNRs are practically the same regions of the crystal. A similar conclusion has recently been derived theoretically by means of first principles-based simulations [11]. Furthermore, it was suggested that the nanosize CORs constitute the necessary condition for the appearance of PNRs and, consequently, the relaxor behavior should not be observed in those crystals where CORs are absent or where their size is much larger than the size of PNRs. This suggestion was supported by the experiments showing that increasing the CORs size in the $Pb(Sc_{1/2}Nb_{1/2})O_3$ (PSN), $Pb(Sc_{1/2}Ta_{1/2})O_3$ and $Pb(In_{1/2}Nb_{1/2})O_3$ relaxors (*e.g.* by means of high-temperature annealing) or elimination of CORs from PMN by means of B-site substitution with Ti leads to the vanishing of characteristic relaxor properties (diffuseness of dielectric constant peak and relaxor dispersion) [10].

An entirely different picture appeared as a result of the analysis of the elastic and quasielastic neutron scattering data [12]. It was suggested that PNRs which are formed inside CORs are pinned by the local compositional order

and therefore are static. Dynamic PNRs that are able to contribute to the relaxation phenomena appear and grow in the whole crystal.

To verify directly the validity of the different models mentioned above, simultaneous examination of the compositional and polar orderings in the same nanoscale region of the crystal is required, which turns out to be a difficult experimental task. Most experimental techniques used to study relaxors, *e.g.* diffuse neutron and X-ray scattering, Raman and Brillouin light scattering, nuclear magnetic resonance (NMR), dielectric spectroscopy, etc. can determine (directly or indirectly) certain characteristics of PNRs, but are hardly able to locate them in space. Accordingly, few experimental data have been available so far in this field. Contradictory results were reported based on the transmission electron microscopy (TEM): no direct correlation between the size and shape of the CORs and ferroelectric domains was observed in PMN-PST system [13], while the model suggested for PMN implicates small nonpolar CORs inside PNRs of larger size [14]. Besides, the very existence of static (not contributing to the relaxation processes) PNRs in the ergodic relaxor phase was not confirmed unambiguously in experiments. It is not clear if the PNRs observed by TEM are static or dynamic. The reports about static PNRs were based on the data of neutron spin-echo spectroscopy [15, 16] and NMR [17] which are restricted by certain time scales (10^{-9} s and 10^{-4} s, respectively). Therefore "static" PNRs revealed in these investigations in the ergodic relaxor phase may appear quasistatic in fact and contribute to the low-frequency part of the broad relaxation spectrum observed by the dielectric spectroscopy. This particular model was adopted by the authors of the recent neutron diffuse scattering investigation [16], who interpreted the onset of static scattering component below 400 K in PMN as a result of the slowing-down of dynamic PNRs and suggested that PNRs become truly static only below $T_f \sim 200$ K *i.e.* in the nonergodic relaxor phase.

In the present work we investigate the relation between CORs and PNRs through comparing the structure and properties of PMN-based solid solutions in which the size and concentration of COR are modified by means of chemical doping and special thermal treatment. We demonstrate that there is no significant influence of the morphology of CORs on the dynamics of PNRs. It is found that static PNRs whose reorientations do not contribute to the dielectric relaxation can exist in the ergodic relaxor phase and that the dynamic PNRs are present even in those crystals where CORs are absent.

Observation of static and dynamic PNRs in $0.9Pb(Mg_{1/3}Nb_{2/3})O_3-0.1PbTiO_3$ crystals by means of piezoresponse force microscopy

In this section we analyze the results of our piezoresponse force microscopy (PFM) investigations of dipole dynamics in the ergodic relaxor phase of $0.9Pb(Mg_{1/3}Nb_{2/3})O_3-0.1PbTiO_3$ (PMN-10PT) crystals. The TEM studies of this perovskite solid solution reveal CORs with the size of about 3 nm [18]. The spontaneous (*i.e.* without application

of external field) ferroelectric phase transition is found by X-ray diffraction below room temperature at $T_C \cong 280$ K [19], while the characteristic relaxor peak of the dielectric constant occurs at 310 K (at 1 kHz). Strong dielectric dispersion observed around room temperature in an extremely wide frequency range [20] suggests the existence of relaxing PNRs, which makes this crystal a convenient object for studying the PNR dynamics.

With the PFM technique one can measure piezoelectric response locally (typically within an area of $\sim 30 \times 30$ nm^2). As the piezoelectric response is proportional to the spontaneous or induced long-living polarization (P), the local values of magnitude and direction of P can be estimated. In scanning regime the spatial distribution of the polarization (domain structure) near the surface of crystal can be mapped (see Ref. [20] for experimental details). The scan obtained on the PMN-10PT crystal is shown in Fig. 1a and b which represent the images typically observed in the ergodic phase of relaxors [21, 22]. One can see the labyrinthine domains having the characteristic size of ~ 200 nm. The values of P inside these domains are comparatively small (much smaller than in the domains of a typical normal ferroelectric phase in perovskites) but stable: the domain structure remains unchanged when measured in the time intervals of many hours. Upon heating the amplitude of the piezoresponse in the domains is gradually decreases.

Applying a focused depth-resolved synchrotron X-ray diffraction technique which is able to probe the local crystal structure with the submicrometre spatial resolution, we studied the sample shown in Fig. 1 and confirmed that the crystal structure remains cubic, and practically independent of the distance from the crystal surface (see Ref. [20] for details). The existence of polar domains in the cubic (*i.e.* non-ferroelectric) phase is not generally expected and requires explanation. As their size is much larger than the size of PNR, every domain must contain a large number of PNRs. On the other hand, PNRs are too small to be resolved by PFM. Therefore, the labyrinthine domains are in fact frozen spatial fluctuations of polarization caused by the density fluctuations of PNRs having dipole moment directions up or down. While PFM samples only near-surface regions, we believe (though we cannot prove it unambiguously by now) that these labyrinthine domains cross the entire thickness of the crystal.
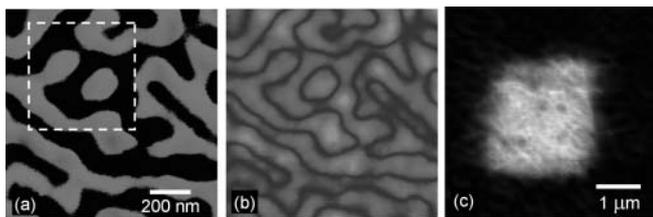
Fig. 1. PFM images of the (001) surface of a PMN-10 PT crystal before [(**a**) and (**b**)] and immediately after (**c**) application of a *dc* bias pulse of 10 V (different location). (a) Phase image. Black and white areas are the domains in which the [001] component of the polarisation, P_Z, is positive and negative, respectively. (b) and (c) Amplitude images. Dark areas correspond to small values of P_Z magnitude; the brighter the area, the larger the P_Z magnitude.
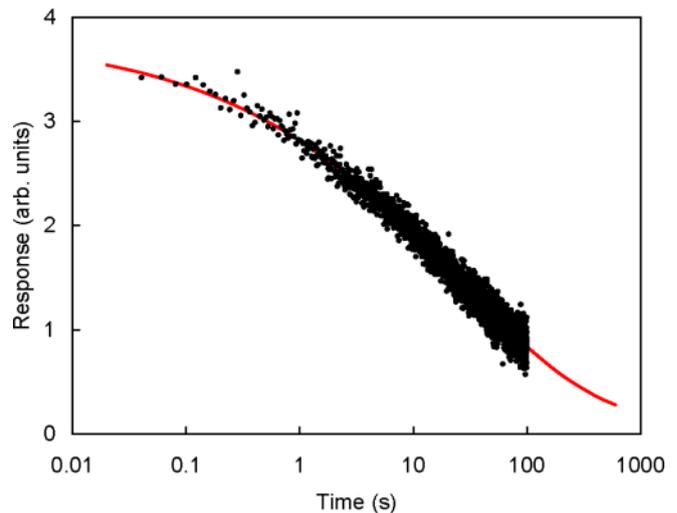

Fig. 2. Relaxation of the vertical piezoresponse (proportional to local polarization) measured using PFM in the PMN-10PT crystal at room temperature after switching off the *dc* bias signal of 10 V applied for 1 s. Dots are the experimental data; solid line is the fitted KWW dependence with $\tau = 25$ s and $\beta = 0.36$.

A long-living polarization which is several times larger can be induced by the bias field applied to the sample with the help of the PFM tip, as shown in Fig. 1c. This induced polarization (P_{ind}) relaxes with time to the value observed before poling so that practically the same labyrinthine domain configuration finally restores. Both the increase of polarization upon switching on the bias and the drop of the polarization upon switching off follow the Kohlrausch-Williams-Watts (KWW) relaxation law, $P_{ind} \sim \exp\left(-t/\tau\right)^{\beta}$. The example of such behavior for one of the points is shown in Fig. 2. While mesoscopic heterogeneities of the relaxation dynamics were observed (100–200 nm regions with comparatively large and small values of τ) [20, 23] the average τ was found to be close to the value derived from the dielectric relaxation spectrum. This suggests that the mechanism of the relaxation observed by PFM and in dielectric spectroscopy is the same, namely, the reorientations of the dynamic PNRs.

One can suggest at least two ways to explain the origin of the static labyrinthine domains. The first explanation is that the dynamic PNRs in these domains possess preferred orientations due to the influence of local electric fields. These fields caused by compositional disorder and other structural defects are quenched, *i.e.*, do not vary with time so that after switching off the electric bias the PNRs relax to the configuration prescribed by the configuration of the local fields. Alternatively, truly static PNRs may be responsible for labyrinthine domains. To discriminate between these two possibilities we applied switching spectroscopy PFM [24].

Switching spectroscopy PFM makes it possible to determine the configuration of local quenched electric fields in the material. This can be done by local measurements of the ferroelectric hysteresis loops. It is known that the ferroelectric hysteresis loops measured in bulk samples by conventional techniques (*e.g.* Sawyer-Tower) may be shifted along the field axis when an internal bias field is present (*e.g.* due to preferential orientation of defects). We observed such a kind of shifts for local loops measured with PFM [24]. Considering the direction and magnitude
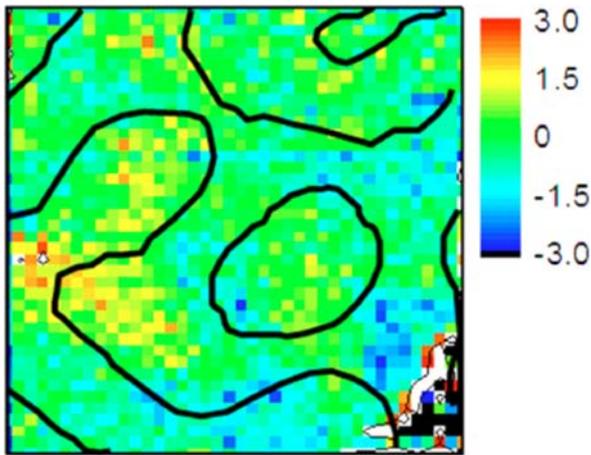
Fig. 3. The map of local quenched electric fields derived from switching spectroscopy PFM of the area of the PMN-10 PT crystal outlined in Fig. 1(a) by the dashed-line square. The pixel size is 12.5 nm. The black lines are the contour map overlay representing the boundaries of the labyrinthine domains.
Reproduced with permission from [24]. Copyright 2009, American Institute of Physics.

of the shift, the direction and relative magnitude of the quenched local electric fields at different points of the crystal were determined and the corresponding map is shown in Fig. 3. One can see mesoscopic ($\sim$100–200 nm) spatial fluctuations of the field, while the value averaged over the whole sample remains practically zero. The configuration of these spatial fluctuations reveals no correlation with the configuration of the labyrinthine domains (which are shown in Fig. 3 as a contour map). This means that the formation of the labyrinthine domains cannot be explained by the alignment of dynamic PNRs in built-in random electric fields. Neither is there a correlation between the labyrinthine domain structure and the other characteristics of local ferroelectric loops (switchable polarization, work of switching, etc.) [24], which further confirms that they are from different origins and explains the relative independence of the bias-induced polarization

(coming from the reorientations of dynamic PNRs, and, possibly, the growth of the PNR size) and the labyrinthine domains (created by static PNRs). These are truly static PNRs: their directions cannot be reoriented by thermal motion and they do not take part in the relaxation processes.

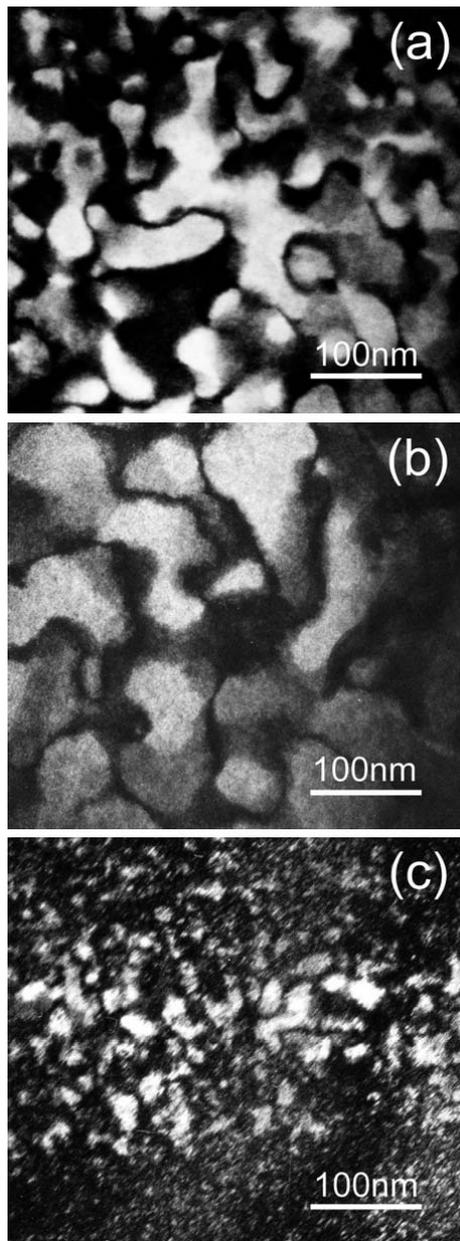## Phase transitions and relaxation in doped $Pb(Mg_{1/3}Nb_{2/3})O_3$ with different sizes of CORs

While the results of PFM experiments described in the previous section suggest the coexistence of static and dynamic PNRs in the ergodic relaxor phase, they can say little about the connection between PNRs and CORs: compositional ordering does not change the cubic point symmetry of the structure and, therefore, cannot influence directly the piezoelectric response. To reveal possible connection indirectly we compared the PNR-related properties in PMN where the size of CORs is about 2–5 nm and in the chemically modified PMN crystals and ceramics with CORs of various sizes. The degree of compositional disorder averaged over the whole sample (S) was determined from relative intensity of fundamental and superstructure X-ray diffraction reflections while the size of CORs was estimated from the TEM micrographs. The compositions studied are listed in Table 1, which include pure PMN crystals and ceramics, La-doped PMN crystals (PLMN) where a doping level as low as 2 at% induced comparatively large ($\sim$100 nm) CORs [25] and several PMN-based ceramic solid solutions where large-size CORs and detectable S appeared only after special high-temperature treatment (slow cooling after sintering, see Ref. [26] for details). Selected TEM images in Fig. 4 demonstrate CORs in partially ordered ceramics.

In Fig. 5 the dielectric permittivity is compared in compositionally disordered PMN crystals and partially ordered PLMN crystals. The data are normalized for convenience. One can see that the shape of the dielectric peak and the dielectric dispersion is practically unaffected by compositional ordering: the curves for the two samples coincide

Table 1. Comparison of the parameters describing dielectric relaxation and ferroelectric phase transition in compositionally disordered and partially ordered pure and modified PMN crystals and ceramics.[a]

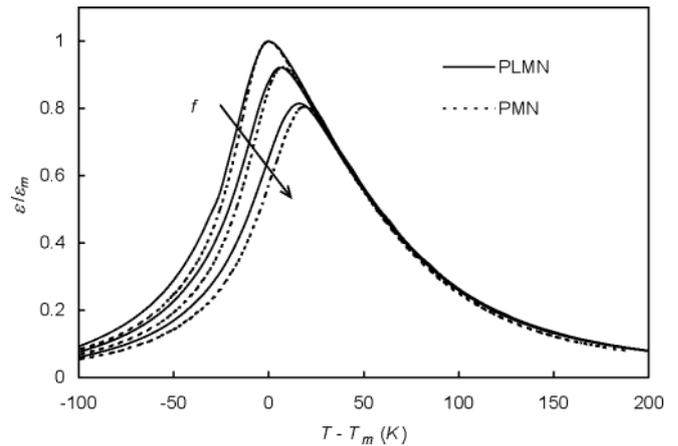| Composition	S	$10^{-2}\,\varepsilon_m$ at 1 kHz	T_m at 1 kHz (K)	δ (K)	T_f (K)	T_β (K)	$10^{15}\,\tau_0$ (s)	E_τ (K)	β_0	E_β (K)	T_C (K)	W (K)
Crystal PMN	0	200	265	41	213	210	16	810	0.43	42	215	
Ceramics PMN	0	174	264	45	217	216	13	831	0.48	49	201	0.8
Crystal 0.98 PMN−0.02 La(Mg$_{2/3}$Nb$_{1/3}$)O$_3$	0.44	101	261	45	192		11	1080				
Ceramics 0.97 PMN−0.03 La(Mg$_{2/3}$Nb$_{1/3}$)O$_3$	0	72	217	77	148	147	0.44	1445	0.39	43	143	13
	0.4	68	218	78	154	141	1.4	1247	0.39	48	145	10
Ceramics 0.94 PMN−0.06 Pb(Sc$_{1/2}$Nb$_{1/2}$)O$_3$	0	195	270	46	224	211	26	682	0.44	62	213	1.3
	0.4	188	269	45	228	219	17	743	0.48	50	212	0.6
Ceramics 0.96 PMN−0.04 Pb(Mg$_{1/2}$W$_{1/2}$)O$_3$	0	120	251	60	185	180	2.0	1086	0.36	52	172	14
	0.4	147	255	53	184	183	0.16	1500	0.40	62	174	8
Crystal 0.45 PMN−0.55 PbTiO$_3$	0		521	20							521	

a: Typical uncertainties are ± 2 K, ± 3 K, ± 5 K, ± 100 K, ± 0.03 and ± 7 K for δ, T_f, T_β, E_τ, β_0 and E_β, respectively.

Fig. 5. Normalized dielectric constant ($\varepsilon/\varepsilon_m$) at three different frequencies, 10 Hz, 1 kHz and 100 kHz, as a function of ($T - T_m$) measured in the [100] direction in compositionally disordered PMN and partially ordered ($S = 0.44$) 0.98 PMN$-$0.02 La(Mg$_{2/3}$Nb$_{1/3}$)O$_3$ (PLMN) crystals. T_m and ε_m are the temperature and the magnitude of the $\varepsilon(T)$ maximum at 10 Hz, respectively.

Fig. 4. Compositionally ordered domains in partially ordered ($S = 0.4$) ceramics: (**a**) 0.97 PMN$-$0.03 La(Mg$_{2/3}$Nb$_{1/3}$)O$_3$, (**b**) 0.94 PMN$-$0.06 Pb(Sc$_{1/2}$Nb$_{1/2}$)O$_3$ and (**c**) 0.96 PMN$-$0.04 Pb(Mg$_{1/2}$W$_{1/2}$)O$_3$. The dark field TEM images are formed with the ($^1/_2$ $^1/_2$ $^1/_2$) superlattice spot in the $\langle 110 \rangle$-zone axis selected area electron diffraction pattern.

and a small discrepancy is observed only in the low-temperature range. On the other hand, the height of the peak, ε_m, is much smaller in PLMN than in PMN (see Table 1), which can be attributed mainly to the composition variation (due to La doping) rather than to the modified ordering. Indeed, the difference in ε_m between the disordered and ordered ceramic samples of the same composition is comparatively small in all cases (see Table 1).

The dielectric response in the ergodic relaxor phase (*i.e.* in the temperature range of the permittivity maximum) is believed to be determined mainly by the reorientations of the dipole moments of dynamic PNRs. The other contributions related to soft phonons, motion of the boundaries of (static and dynamic) PNR, etc. also exist [9, 27, 28]. In particular, different polar-phonon modes related to CORs and

compositionally disordered regions were revealed in the IR reflectivity spectra of 0.65 Pb(Mg$_{1/3}$Nb$_{2/3}$)O$_3$$-$0.35 PbTiO$_3$ ceramics [29]. However, in PMN these additional dielectric contributions are comparatively small and become significant only at low temperatures, where flipping of dynamic PNRs is frozen. Therefore, the observed similarity of dielectric peaks in PMN and PLMN means that the subsystem of dynamic PNRs has no relation to the compositionally ordered regions. Small difference in the low-temperature behaviour is probably related to some changes in the subsystem of static PNRs and/or phonon spectrum.
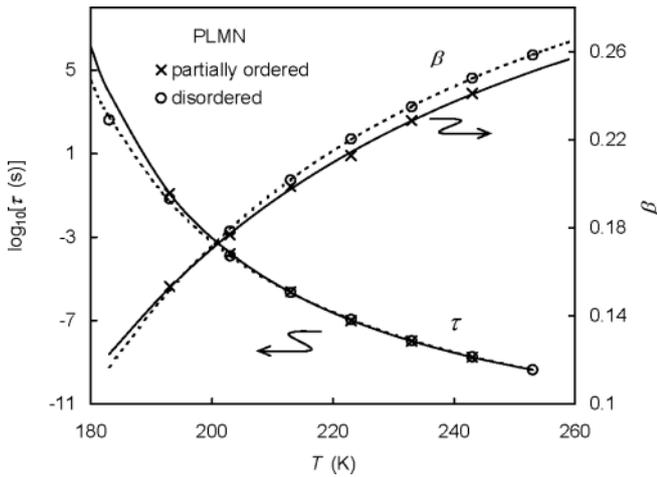
To quantitatively characterise the behaviour the experimental data were fitted to the formulae which are proven to be able to fully describe the dielectric response of flipping PNRs in the ergodic phase of relaxors [3, 9]. The high-temperature (frequency-independent) slope of the $\varepsilon(T)$ peak was fitted to the quadratic relation

$$\frac{\varepsilon_A}{\varepsilon} = 1 + \frac{(T - T_A)^2}{2\delta^2} , \tag{1}$$

where T_A and ε_A are the fitting parameters standing for the extrapolated values of the height and position of the static dielectric constant peak, *i.e.* $T_A \equiv T_m$ ($f = 0$) and $\varepsilon_A \equiv \varepsilon_m$ ($f = 0$), and δ is the diffuseness parameter characterizing the width of the peak. The dielectric dispersion in the temperature range of the peak was found to follow the KWW relaxation law which includes two parameters, namely, the characteristic relaxation time, τ, and the stretching exponent $0 \leq \beta \leq 1$ (the value $\beta = 1$ corresponds to the Debye relaxation and a decreasing β indicates widening of the relaxation time distribution in the frequency domain). The temperature dependences of these relaxation parameters in all compositions studied (Fig. 6 gives some examples) follow the Vogel-Fulcher-type relationships:

$$\tau = \tau_0 \exp\left[\frac{E_\tau}{(T - T_f)}\right] , \tag{2}$$

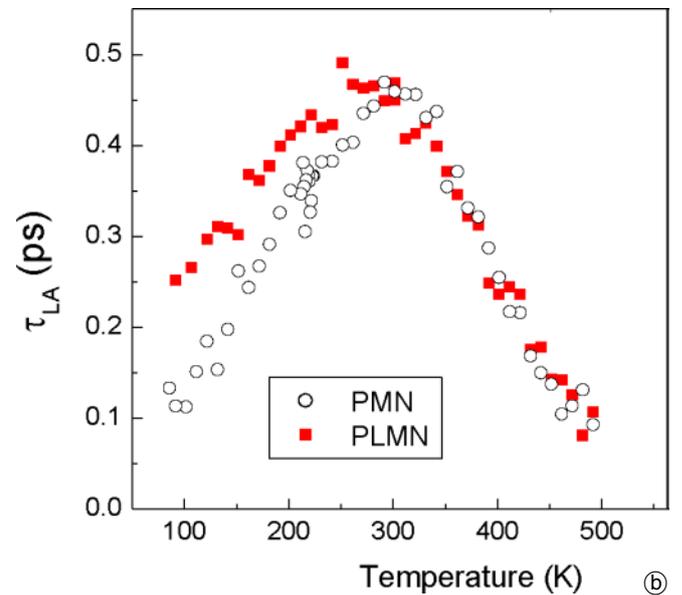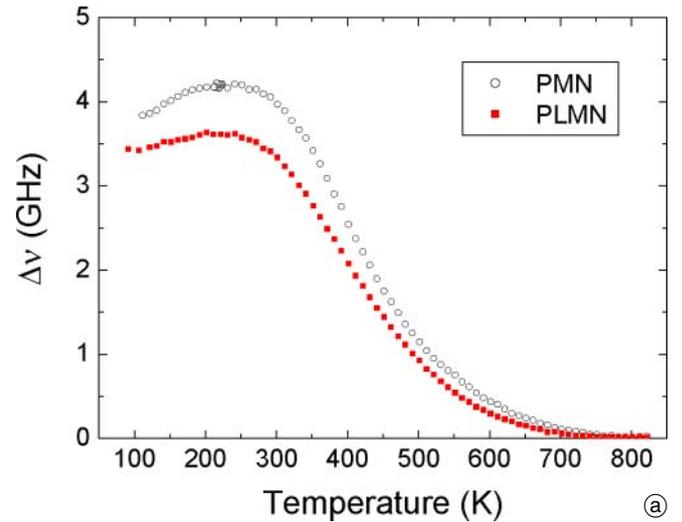$$\beta = \beta_0 \exp\left[-\frac{E_\beta}{(T - T_\beta)}\right] . \tag{3}$$

Fig. 6. Temperature dependences of the relaxation parameters in disordered and partially ordered ($S = 0.4$) 0.97 PMN−0.03 La(Mg$_{2/3}$Nb$_{1/3}$)O$_3$ ceramics. The fits to the Vogel-Fulcher relationships [Eqs. (2) and (3)] are shown by dashed and solid lines for disordered and partially ordered samples, respectively.

The parameters T_f and T_β ($T_f \cong T_\beta$) are the extrapolated temperatures at which the characteristic relaxation time and the width of the relaxation spectrum become infinite, respectively, signifying the freezing of the spectrum. The best-fit relaxation parameters for different compositions are listed in Table 1.

Comparison of the dielectric relaxation characteristics of all the ordered and disordered samples confirms the trends found above by comparison of PMN and PLMN crystals. The parameters δ, which characterize the shape (diffuseness) of the temperature dependence of the static dielectric constant and the Vogel-Fulcher parameters T_f, τ_0, E_τ, T_β, E_β and β_0, which describe the temperature evolution and freezing of the relaxation spectrum, are the same, or almost the same, in the disordered samples as in their partly ordered counterparts. The influence of the compositional order on the magnitude of the dielectric constant (the value of ε_m) is also comparatively small. This behaviour presents a striking contrast to the behaviour of Pb(B$'_{1/2}$B$''_{1/2}$)O$_3$-type relaxors where compositional ordering causes significant variations in the temperature and diffuseness of dielectric peak, as well as in the dielectric dispersion [2, 4−6].

The dielectric spectroscopy data are related to frequencies lower than ∼1 MHz and therefore provide information concerning the relaxation at comparatively low temperatures where PNR dynamics becomes comparatively slow. The relaxation at higher frequency range was studied by means of Brillouin scattering [30]. The Brillouin spectra were collected in PMN and PLMN crystals in backward scattering geometry and probed the longitudinal acoustic (LA) phonons propagating in the [100] pseudocubic direction. Interaction of PNRs with acoustic phonons leads to a significant decrease in sound velocity and consequently to a decrease in the value of the related Brillouin frequency shift (ν_B) as compared to the shift which would have been observed without PNRs (ν_∞). Besides, if the relaxation time of PNRs is comparable with the reciprocal acoustic mode frequency, additional acoustic damping appears resulting in widening of the Brillouin peak.


Fig. 7. Comparison of the LA mode behaviour in the compositionally disordered PMN and partially ordered ($S = 0.44$) 0.98 PMN−0.02 La(Mg$_{2/3}$Nb$_{1/3}$)O$_3$ crystals in terms of the temperature dependences of (**a**) the part of the Brillouin frequency shift related to the interaction with PNRs and (**b**) the relaxation time calculated from the width of the Brillouin peak according to Eq. (4).

Figure 7a shows the temperature dependences of the additional frequency shift, $\Delta\nu = \nu_\infty - \nu_B$. The ν_∞ values were estimated by means of extrapolation of linear $\nu_B(T)$ dependence observed at $T > T_B$ (where PNRs are absent) to lower temperatures. The relaxation time shown in Fig. 7b was calculated using the relation

$$\tau_{LA} = \frac{\Gamma_B - \Gamma_\infty}{2\pi(\nu_\infty^2 - \nu_B^2)}, \tag{4}$$

where Γ_B is the Brillouin peak full-width-at-half-maximum and Γ_∞ is the constant value of Γ_B observed at $T > T_B$ (see Ref. [30] for more details). It is evident that both $\Delta\nu$ which should depend on the concentration of PNRs, and τ_{LA} which is determined by the PNRs relaxation times are practically the same in the ordered and disordered samples almost in the whole temperature range of ergodic relaxor phase.
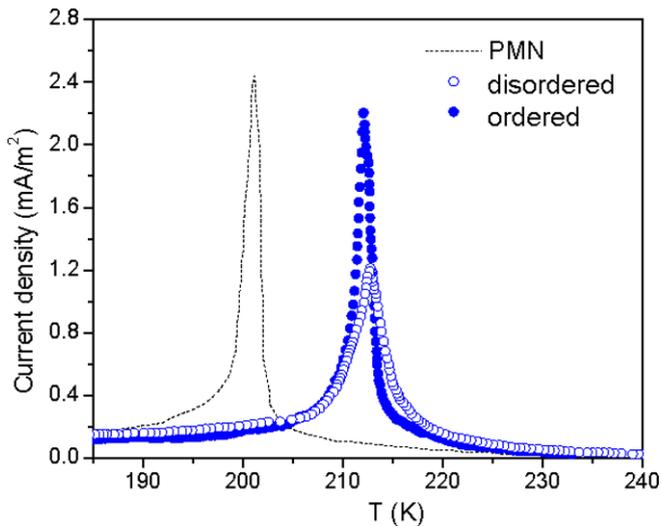
Fig. 8. Thermal depolarization current measured during zero-field heating of disordered and partially ordered ($S = 0.4$) 0.94 PMN−0.06 Pb(Sc$_{1/2}$Nb$_{1/2}$)O$_3$ ceramics after cooling at 10 kV/cm. The current for pure PMN ceramics obtained under the same conditions is shown by dashed line for comparison.

Besides the small-signal dielectric measurements the response to a large external dc electric field was studied. It is known that this field, being larger than certain threshold value, can induce in relaxors a metastable ferroelectric phase at $T < T_f$ [31]. We studied this phase transition by measuring the pyroelectric current on heating (without field) for the samples in which the ferroelectric phase has been induced by field-cooling through T_f. The example for Sc-doped ceramics is shown in Fig. 8. The temperature of the transition from ferroelectric to ergodic relaxor phase (T_C) was determined as the temperature of the current peak. To characterize the diffuseness of the transition the half-width of the depolarization current peak at $^2/_3$ maximum (W) was measured and presented in Table 1. One can see that the compositional disorder has practically no effect on the transition temperature T_C, but significantly increases the diffuseness of the transition. The same conclusion has been made based on the shape of the temperature dependences of the remnant polarisation determined from the ferroelectric hysteresis loops [26].

Phase transitions and relaxation in doped Pb(Mg$_{1/3}$Nb$_{2/3}$)O$_3$ without CORs

In the previous section we discussed relaxors in which the size of CORs was increased as compared to the pure PMN. In some cases, however, doping can lead to a size decrease and even complete elimination of CORs. In particular, this happens in $(1 − x)$PMN−xPbTiO$_3$ solid solutions where CORs disappear at x exceeding ∼0.4, as found by transmission electron microscopy [18] and confirmed by synchrotron X-ray scattering studies [32]. The question was naturally raised whether PNRs still exist when CORs are absent. To answer this question, we studied the 0.45 PMN−0.55 PbTiO$_3$ (PMN-55PT) crystal. One particular feature of this crystal is that the ferroelectric phase appears spontaneously upon cooling (*i.e.* without
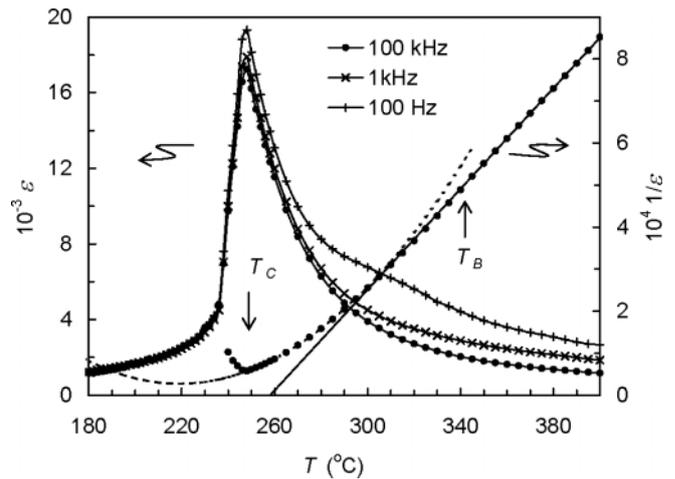

Fig. 9. Temperature dependences of the dielectric constant measured in a PMN-55PT crystal at different frequencies in the [001] direction. Solid and dashed lines represent fitting of experimental data to the Curie-Weiss law and the quadratic law, Eq. (1), respectively.

poling electric field) through sharp phase transition at $T_C = T_m = 521$ K [33].

Our dielectric and light scattering experiments revealed in a wide temperature range above T_C the behaviour typically observed in relaxors and usually attributed to the existence of PNRs. As can be seen in Fig. 9, the dielectric constant follows the Curie-Weiss law, $\varepsilon = C/(T − T_{CW})$, at high temperatures with $T_{CW} > T_m$ (a feature typical of relaxors). The deviation from this law is observed in relaxors at the Burns temperature. In PMN-55PT the deviation is found at about 620 K. This is practically the same deviation temperature as in pure PMN and it can be interpreted as the Burns temperature, T_B. In the interval of $T_m < T < T_B$ the characteristic of the ergodic relaxor phase quadratic relation for the dielectric constant, Eq. (1), is valid with the parameters listed in Table 1.

The Brillouin spectra of PMN-55PT and their temperature variations also show typical relaxor features. Upon approaching T_C from above, the strong central peak ap-
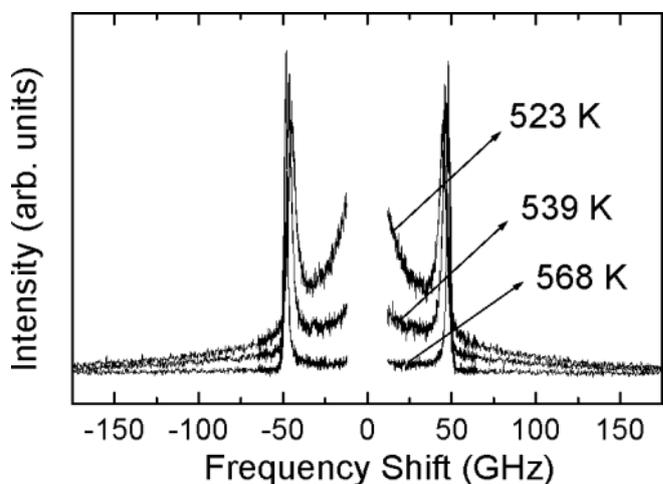
Fig. 10. Brillouin spectra measured in the (100)-oriented PMN-55PT crystal plate in a backward scattering geometry at three different temperatures above $T_C = 521$ K. The central peak increasing with decreasing temperature is found alongside with the Brillouin doublet from LA mode.
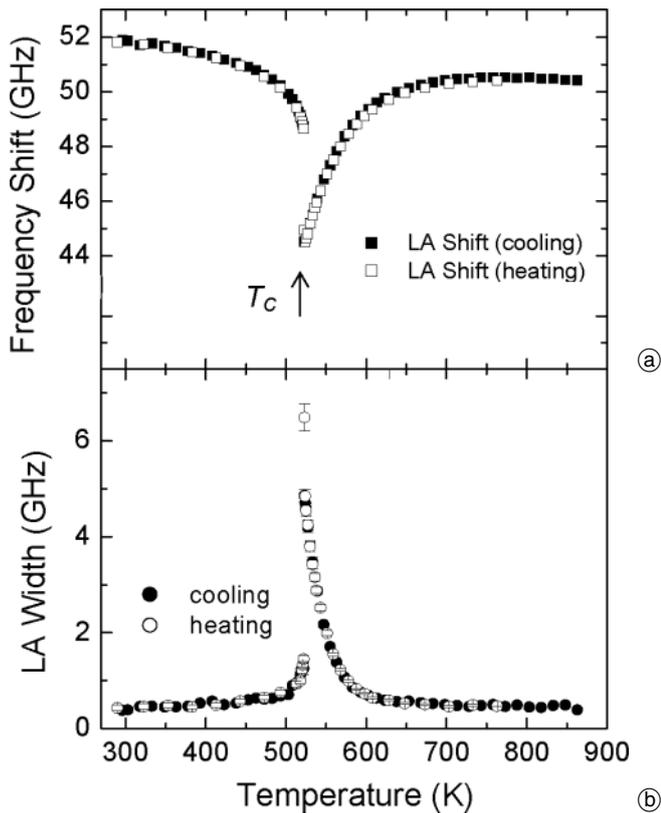
Fig. 11. The LA mode behaviour in the PMN-55PT crystal. The temperature dependences of (**a**) the Brillouin frequency shift and (**b**) the Brillouin peak full-width-at-half-maximum measured on cooling and heating.

pears at $T < T_B$ and grows (Fig. 10), the LA mode substantially softens and the width of the peak increases, signalling increasing acoustic damping (Fig. 11). All these features are related to the existence of the *dynamic* PNRs (see Ref. [34] for more details). The relaxation time, τ, of the PNR motion derived from the central peak (it is inversely proportional to the peak width) increases upon cooling in the ergodic relaxor phase, following the relation $\tau \propto (T - T_0)^{-1}$ characteristic of order-disorder phase transitions [34]. However, at T_C the value of $1/\tau$ is still much larger than the largest frequency used in our dielectric measurements. Accordingly, the conventional relaxor dielectric dispersion is not observed in the ergodic relaxor phase (Fig. 9) and the maximum in the temperature dependence of ε appears not because of the dielectric dispersion (as *e.g.* in pure PMN) but because of the phase transition. For this reason T_m is practically independent of frequency and equals T_C.

Further discussion and conclusions

The experiments reviewed in the present paper are consistent with the model in which both static and dynamic PNRs exist in the ergodic relaxor phase. The evidence of the static PNRs was obtained with the help of PFM measurements while the characteristics of the dynamic PNRs were studied with PFM, dielectric spectroscopy and Brillouin scattering. It is shown that the presence of CORs is

not the necessary condition for the PNRs formation: PNRs are formed even in completely compositionally disordered PMN-55PT crystals. Furthermore, no correlation between CORs and dynamic PNRs was observed: the dynamic characteristics of doped PMN relaxors in a wide frequency range from 10^{-2} to 10^{12} Hz were independent of the COR size. This result is consistent with the previous reports [35, 36] that the degree of compositional ordering had no substantial effect on the dielectric properties and phonon dynamics of $Pb(Mg_{1/3}Ta_{2/3})O_3$, which seems to be characteristic of the $Pb(B'_{1/3}B''_{2/3})O_3$ perovskite relaxors, contrasting with the $Pb(B'_{1/2}B''_{1/2})O_3$ perovskites. This difference is related to the fact that in the fully ordered state of $Pb(B'_{1/2}B''_{1/2})O_3$ two B-site sublattices exist, each being filled by a certain type of B-cations (B' or B'') so that the translational symmetry is maintained, while in the $Pb(B'_{1/3}B''_{2/3})O_3$ case even in the state of the maximal compositional order one of the two sublattices is filled by the disordered mixture of B' and B'' ions and the translational symmetry is still absent.

Our results support the idea that dynamic PNRs may exist in the ergodic relaxor phase both in compositionally disordered regions and inside CORs. Indeed, the effects which are expected to be dependent on the average concentration of PNRs, such as the magnitude of the dielectric constant or the acoustic phonon softening, are nearly the same in the samples with large and small fractions of compositionally ordered regions. On the other hand, in 0.4PMN-0.6PT crystals (very close to our PMN-55PT composition) where CORs are absent, the static PNRs were not found in the diffuse neutron scattering experiments either [37]. This seems to suggest that static PNRs may appear only inside CORs. Furthermore, we showed [25] that the growth of CORs (in PLMN as compared to PMN crystals) can lead to the growth of static PNRs and they become so large to be observed in routine X-ray diffraction experiments (a mixture of cubic and rhombohedral phases was found in the PLMN crystals at room temperature).

Another remarkable conclusion is that the COR morphology, which has no significant effect on the dynamics of PNRs in the ergodic relaxor phase, influences greatly the ferroelectric phase transition. As discussed elsewhere [26] this behaviour can be understood in the framework of the phenomenological kinetic model of diffuse phase transitions in disordered crystals [38, 39], which considers the dipole structure evolution in relaxor ferroelectrics as the process consisting of two comparatively independent steps: creation of PNRs in a wide temperature range of the ergodic relaxor phase and their thermally activated growth into large ferroelectric domains at T_C.

Although a consistent picture of the relaxor-ferroelectric nanostructure is presented in this article, a number of conclusions were derived, as already mentioned above, based on indirect data only. The range of compositions studied is also rather limited. Therefore, more research is needed to ensure a thorough understanding of the relations between compositional order/disorder and dipole dynamics in $Pb(B'_{1/3}B''_{2/3})O_3$ perovskite relaxors. These data would be indispensable for the construction of any successful theories of relaxor ferroelectrics.

References

[1] Cross, L. E.: Relaxor Ferroelectrics. Ferroelectrics **76** (1987) 241–267.

[2] Cross, L. E.: Relaxor Ferroelectrics: an overview. Ferroelectrics **151** (1994) 305–320.

[3] Bokov, A. A.; Ye, Z.-G.: Recent progress in relaxor ferroelectrics with perovskite structure. J. Mater. Sci. **41** (2006) 31–52.

[4] Stenger, C. G. F.; Burggraaf, A. J.: Order-disorder reaction in the ferroelectric perovskites $Pb(Sc_{0.5}Nb_{0.5})O_3$ and $Pb(Sc_{0.5}Ta_{0.5})O_3$. Phys. Status Solidi A **61** (1980) 653–664.

[5] Bokov, A. A.; Rayevskii, I. P.; Smotrakov, V. G.: Influence of ion ordering at lattice sites on the properties of $Pb_2B'B''O_6$ ternary oxides. Fiz. Tverd. Tela **25** (1983) 2025–2028 [English translation: Sov. Phys. Sol. State **25**, (1983) 1168–1177].

[6] Chu, F.; Setter, N.; Tagantsev, A. K.: The spontaneous relaxor-ferroelectric transition of $Pb(Sc_{0.5}Ta_{0.5})O_3$. J. Appl. Phys. **74** (1993) 5129–5134.

[7] Bokov, A. A.; Ye, Z.-G.: Universal relaxor polarization in $Pb(Mg_{1/3}Nb_{2/3})O_3$ and related materials. Phys. Rev. B. **66** (2002) 064103.

[8] Pirc, R.; Blinc, R.: Freezing dynamics of relaxor ferroelectrics and dipolar glasses. Ferroelectrics **379** (2009) 254–258.

[9] Bokov, A. A.; Ye, Z.-G.: Double freezing of dielectric response in relaxor $Pb(Mg_{1/3}Nb_{2/3})O_3$ crystals. Phys. Rev. B. **74** (2006) 132102.

[10] Randall, C. A.; Bhalla, A. S.: Nanostructural-property relations in complex lead perovskites. Jpn. J. Appl. Phys. **29** (1990) 327–333.

[11] Burton, B. P.; Cockayne, E.; Waghmare, U. V.: Correlations between nanoscale chemical and polar order in relaxor ferroelectrics and the lengthscale for polar nanoregions. Phys. Rev. B **72** (2005) 064113.

[12] Vakhrushev, S.: Polar nanoregions and nanodomains in relaxors. Abstract Book of the 11th European Meeting on Ferroelectricity, Bled, Slovenia, 2007, p. 219.

[13] Farber, L.; Davies, P.: Influence of cation order on the dielectric properties of $Pb(Mg_{1/3}Nb_{2/3})O_3-Pb(Sc_{1/2}Nb_{1/2})O_3$ relaxor ferroelectrics. J. Am. Ceram. Soc. **86** (2003) 1861–1866.

[14] Yoshida, M.; Mory, S.; Yamamoto, N.; Uesu, Y.; Kiat, J. M.: TEM observation of polar domains in relaxor ferroelectric $Pb(Mg_{1/3}Nb_{2/3})O_3$. Ferroelectrics **217** (1998) 327–333.

[15] Vakhrushev, S.; Ivanov, A.; Kulda, J.: Diffuse neutron scattering in relaxor ferroelectric $PbMg_{1/3}Nb_{2/3}O_3$. Phys. Chem. Chem. Phys. 7 (2005) 2340–2345.

[16] Stock, C.; Van Eijck, L.; Fouquet, P.; Maccarini, M.; Gehring, P. M.; Xu, G.; Luo, H.; Zhao, X.; Li, J.-F.; Viehland, D.: Interplay between static and dynamic polar correlations in relaxor $Pb(Mg_{1/3}Nb_{2/3})O_3$. Phys. Rev. B. **81** (2010) 144127.

[17] Blinc, R.: Polar nano-clusters in relaxors on the atomic level. Ferroelectrics. **330** (2006) 1–7.

[18] Hilton, A. D.; Barber, D. J.; Randall, C. A.; Shrout, T. R.: On short range ordering in the perovskite lead magnesium niobate. J. Mater. Sci. **25** (1990) 3461–3466.

[19] Ye, Z.-G.; Bing, Y.; Gao, J.; Bokov, A. A.; Stephens, P.; Noheda, B.; Shirane, G.: Development of ferroelectric order in relaxor $(1-x)Pb(Mg_{1/3}Nb_{2/3})O_3-xPbTiO_3$ $(0 \leqq x \leqq 0.15)$. Phys. Rev. B. **67** (2003) 104104.

[20] Kalinin, S.V.; Rodriguez, B.J.; Budai, J. D.; Jesse, S.; Morozovska, A.N.; Bokov, A.A.; Ye, Z.-G.: Direct evidence of mesoscopic dynamic heterogeneities at the surfaces of ergodic ferroelectric relaxors. Phys. Rev. B. **81** (2010) 064107.

[21] Shvartsman, V. V.; Kholkin, A. L.; Orlova, A.; Kiselev, D.; Bogomolov, A. A.; Sternberg, A.: Polar nanodomains and local ferroelectric phenomena in relaxor lead lanthanum zirconate titanate ceramics. Appl. Phys. Lett. **86** (2005) 202907.

[22] Shvartsman, V. V.; Kholkin, A. L.: Evolution of nanodomains in $0.9Pb(Mg_{1/3}Nb_{2/3})O_3$-$0.1PbTiO_3$ single crystals. J. Appl. Phys. **101** (2007) 064108.

[23] Kalinin, S. V.; Rodriguez, B. J.; Jesse, S.; Morozovska, A. N.; Bokov, A. A.; Ye, Z.-G.: Spatial distribution of relaxation behavior on the surface of a ferroelectric relaxor in the ergodic phase. Appl. Phys. Lett. **95** (2009) 142902.

[24] Rodriguez, B. J.; Jesse, S.; Bokov, A. A.; Ye, Z.-G.; Kalinin, S. V.: Mapping bias-induced phase stability and random fields in relaxor ferroelectrics, Appl. Phys. Lett **95**, (2009) 093904.

[25] Long, X.; Bokov, A. A.; Ye, Z.-G.; Qu, W.; Tan, X.: Enhanced ordered structure and relaxor behaviour of $0.98Pb(Mg_{1/3}Nb_{2/3})O_3$ $-0.02La(Mg_{2/3}Nb_{1/3})O_3$ single crystals. J. Phys. Condens. Matter **20** (2008) 015210.

[26] Zhao, X.; Qu, W.; Tan, X.; Bokov, A. A.; Ye, Z.-G.: Influence of long-range cation order on relaxor properties of doped $Pb(Mg_{1/3}Nb_{2/3})O_3$ ceramics, Phys. Rev. B **79** (2009) 144101.

[27] Rychetsky, I.; Kamba, S.; Porokhonskyy, V.; Pashkin, A.; Savinov, M.; Bovtun, V.; Petzelt, J.; Kosec, M.; Dressel, M.: Frequency-independent dielectric losses (1/f noise) in PLZT relaxors at low temperatures. J. Phys.: Condens. Matter **15** (2003) 6017–6030.

[28] Bovtun, V.; Veljko, S.; Kamba, S.; Petzelt, J.; Vakhrushev, S.; Yakymenko, Y.; Brinkman, K.; Setter, N.: J. Broad-band dielectric response of $PbMg_{1/3}Nb_{2/3}O_3$ relaxor ferroelectrics: Single crystals, ceramics and thin films. J. Eur. Cer. Soc. **26** (2006) 2867–2875.

[29] Bovtun, V.; Kamba, S.; Veljko, S.; Nuzhnyy, D.; Kroupa, J.; Savinov, M.; Vanìk, P.; Petzelt, J.; Holc, J.; Kosec, M.; Amorín, H.; Alguero, M.: Broadband dielectric spectroscopy of phonons and polar nanoclusters in $PbMg_{1/3}Nb_{2/3}O_3$-35%PbTiO_3 ceramics: Grain size effects. Phys. Rev. B 79 (2009) 104111.

[30] Ko, J.-H.; Kim, T. H.; Kojima, S.; Long, X.; Bokov, A. A.; Ye, Z.-G.: Effect of chemically ordered regions on the acoustic behaviors in $Pb(Mg_{1/3}Nb_{2/3})O_3$ studied by Brillouin scattering. J. Appl. Phys. **107** (2010) 054108.

[31] Zhao, X.; Qu, W.; Tan, X.; Bokov, A. A.; Ye, Z. G.: Electric field-induced phase transitions in (111)-, (110)-, and (100)-oriented $Pb(Mg_{1/3}Nb_{2/3})O_3$ single crystals. Phys. Rev. B **75** (2007) 104106.

[32] Tkachuk, A.; Zschack, P.; Colla, E.; Chen, H.: Synchrotron X-ray studies of superlattice ordering in $Pb(Mg_{1/3}Nb_{2/3})O_3$ single crystals doped with PbTiO3. Fundamental Physics of Ferroelectrics, AIP Conference Proceeding, vol. **582**, New York, 2001, 45–54.

[33] Bokov, A. A.; Luo, H.; Ye, Z.-G.: Polar nanodomains and relaxor behaviour in $(1-x)Pb(Mg_{1/3}Nb_{2/3})O_3-xPbTiO_3$ crystals with $x = 0.3-0.5$. Mater. Sci. Eng. B **120** (2005) 206–209.

[34] Ko, J.-H.; Kojima, S.; Bokov, A. A.; Ye, Z.-G.: Light scattering study of acoustic phonon modes and central peaks in $Pb[(Mg_{1/3}Nb_{2/3})_{0.45}Ti_{0.55}]O_3$ single crystals. Appl. Phys. Lett. **91** (2007) 252909.

[35] Akbas, M. A.; Davies, P. K.: Domain growth in $Pb(Mg_{1/3}Ta_{2/3})O_3$ perovskite relaxor ferroelectric oxides. J. Am. Ceram. Soc. **80** (1997) 2933–2936.

[36] Kamba, S.; Nuzhnyy, D.; Velijko, S.; Bovtun, V.; Petzelt, J.; Wang, Y. L.; Setter, N.; Levoska, J.; Tyunina, M.; Macutkevic, J.; Banys, J.: Dielectric relaxation and polar phonon softening in relaxor ferroelectric $PbMg_{1/3}Ta_{2/3}O_3$. J. Appl. Phys. **102** (2007) 074106.

[37] Stock, C.; Ellis, D.; Swainson, I. P.; Xu, G.; Hiraka, H.; Zhong, Z.; Luo, H.; Zhao, X.; Viehland, D.; Birgeneau, R. J.; Shirane, G.: Damped soft phonons and diffuse scattering in 40%$Pb(Mg_{1/3}Nb_{2/3})O_3$-60%$PbTiO_3$. Phys. Rev. B **73**, (2006) 064107.

[38] Bokov, A. A.: Kinetics of a diffuse phase transition in crystals with frozen disorder. Fiz. Tverd. Tela **36** (1994) 36–45 [English translation: Phys. Solid State **36** (1994) 19–30].

[39] Bokov, A. A.: Ferroelectric domains and polar clusters in disordered structures. Ferroelectrics, **190** (1997) 197–202.